Applied Catalysis B: Environmental 258 (2019) 117903

Contents lists available at ScienceDirect

Applied Catalysis B: Environmental

journal homepage: www.elsevier.com/locate/apcatb

Role of Ni^{2+} ions in TiO_2 and Pt/TiO_2 photocatalysis for phenol degradation in aqueous suspensions

Yaru Wang, Jianjun Zhao, Xianqiang Xiong, Shengwei Liu, Yiming Xu*

State Key Laboratory of Silicon Materials and Department of Chemistry, Zhejiang University, Hangzhou 310027, PR China

ARTICLE INFO

Keywords:
Photocatalysis
Semiconductor
Titanium oxide
Nickel ions
Phenol
Mineralization

ABSTRACT

Anatase TiO_2 is the most studied environmental photocatalyst, but its efficiency is still not high enough to enable application. Herein we report a positive effect of Ni^{2+} ions on the photocatalytic reaction in neutral aqueous solution. On addition of 1 mM $Ni(ClO_4)_2$, the rates of phenol oxidation on TiO_2 and 0.5 wt.% Pt/TiO_2 increased by factors of 2.1 and 8.0, respectively. Meanwhile, the formation of organic intermediate was reduced, and the removal of total organic content was enhanced. Interestingly, Ni^{2+} concentration did not change with irradiation time. Moreover, a maximum rate of phenol degradation was observed with Ni^{2+} ions, occupying half the surface of TiO_2 or Pt/TiO_2, where $Ni(OH)^+$ was more active than $Ni(OH)_2$. X-ray photoelectron spectroscopy identified a Ni^{3+} species produced in absence of phenol. A (photo)electrochemical study revealed that Ni^{2+} oxidation was favored over H_2O oxidation, whereas Ni^{2+} and Pt inhibited and facilitated O_2 reduction, respectively. It is proposed that the adsorbed $Ni(OH)^+$ on TiO_2 is oxidized to Ni^{3+} by the photogenerated holes of TiO_2, followed by regeneration through phenol oxidation. The Ni^{2+}-catalyzed organic oxidation then promotes the Pt-catalyzed O_2 reduction, and vice visa, resulting into the greatly improved efficiency of charge separation. This work highlights the possibility of Ni^{2+} ions as the hole mediator of organic oxidation over a semiconductor.

1. Introduction

Semiconductor photocatalysis for energy and environmental use has been extensively studied over the past forth decades. The most applied reactions include water splitting to H_2 and O_2 [1], CO_2 reduction to organics with H_2O as reductant [2], and organic degradation to CO_2 with O_2 as oxidant [3]. These reactions have a common feature. Semiconductor first absorbs photons, and generates pairs of electrons and holes in the conduction and valence bands, respectively. Then these charge carriers migrate onto the surface, reacting with sorbates. Due to the fast recombination of charge carriers, however, the quantum yield of a target reaction is usually low. Although new materials need to be developed [4], the central issue of photocatalysis is how to accelerate the interfacial charge transfer through a simple and economic way.

Among various photocatalysts, TiO_2 is the most studied for environmental use, mainly due to its superior band structures [5,6]. In neutral aqueous solution, the conduction band edge potential of anatase TiO_2 are —0.53 V versus normal hydrogen electrode (NHE) [7], which is more negative than the one-electron oxidation potential of O_2 (—0.33 V *vs*. NHE) [8,9]. The counterpart valence band edge potential is 2.67 V *vs*. NHE, which is more positive than the one-electron reduction potentials of many organic substrates [10]. To improve the quantum efficiency of organic degradation, the surface of TiO_2 is usually modified with a cocatalyst [11]. For example, noble metals such as Pt can catalyze the electron reduction of O_2, and hence promote the hole oxidation of organics [12,13]. In acidic aqueous solution, both Fe^{3+} and Cu^{2+} ions can capture the electrons of TiO_2, improving the efficiency of charge separation for organic oxidation [14,15]. But the reoxidation of Fe^{2+} to Fe^{3+} by O_2 is slow, whereas the reoxidation of Cu^+ to Cu^{2+} by O_2 is efficient only at low concentration. In contrary, Co^{2+} ions can capture the holes of TiO_2 to form a highly reactive $Co^{III/IV}$ for organic oxidation. Without precipitating reagent such as phosphate, however, the $Co^{III/IV}$ species deactivate to Co^{2+}, making Co^{2+} in null cycle, and consequently slowing down the TiO_2-photocatalyzed reaction [16].

In this work, the effect of Ni^{2+} ions on the TiO_2-photocatalyzed degradation of organics is examined. The present work focus on the surface adsorbed Ni^{2+} on TiO_2, which is different from the bulk doped Ni^{2+} in TiO_2 [17]. There is also a debate about Ni^{2+} reduction or oxidation occurring or not on the irradiated TiO_2 [18]. Phenol represents a class of aromatic pollutants, and it is often used as a model substrate to assess the catalyst photoactivity, because it is colorless, and its degradation under light at wavelengths longer than 320 nm result only from the TiO_2-photocatalyed reaction [19]. To accelerate the

* Corresponding author.
E-mail address: Xuym@zju.edu.cn (Y. Xu).

https://doi.org/10.1016/j.apcatb.2019.117903
Received 4 May 2019; Received in revised form 18 June 2019; Accepted 24 June 2019
Available online 14 July 2019
0926-3373/

electron transfer, TiO_2 was also deposited with 0.5% of Pt nanoparticles. On addition of 1 mM $Ni(ClO_4)_2$, interestingly, the rates of phenol degradation on TiO_2 and Pt/TiO_2 increased by factors of 2.1 and 8.0, respectively. But Ni^{2+} concentration in aqueous phase remained unchanged with time, either in the absence or presence of phenol. To understand the role of Ni^{2+}, several experiments were carried out, including the change of Ni valence state on solid, the electrochemical reduction of O_2, and the photoelectrochemical oxidation of phenol and water on a film electrode.

2. Experimental

2.1. Materials

Nickel perchlorate and anatase TiO_2 were purchased from Sigma-Aldrich. Dimethylglyoxime and ammonium peroxydisulfate were purchased from Aladdin, and others from Shanghai Chemicals. Pt/TiO_2 was made by a photochemical method. A suspension (50 mL) containing 18 g/L TiO_2, 2 M CH_3OH, and a certain amount of H_2PtCl_6 was irradiated with a 300 W mercury lamp (300 W) for 3 h. Then the solid was collected, and washed several times with water, and dried at 80 °C. The amount of Pt in Pt/TiO_2 was calculated to be 0.5% weight percent.

2.2. Characterization

X-ray diffraction (XRD) patterns were recorded on a D/max-2550/PC diffractometer (Rigaku). Transmission electron microscopy (TEM) was recorded on a JEM-2100 F field-emission instrument. Diffuse reflectance spectra (DRS) were recorded on a Shimadzu UV-2600 with $BaSO_4$ as reference. Reflectance (R) was transferred into Kubelka–Munk absorbance (F_R), equal to $(1–R)^2/(2R)$. Adsorption isotherms of N_2 on solid were measured at 77 K on a Micromeritics ASAP2020 apparatus. X-ray photoelectron spectroscopy (XPS) spectra were recorded on a Kratos AXIS UItra DLD spectrometer, followed by calibration with C 1s at 284.6 eV.

2.3. Photocatalysis and analysis

Experiments were carried out on a photochemical apparatus (Nanjing XuJiang Power Plant, China). Unless stated otherwise, reactions were performed at 25 °C under fixed initial conditions (0.43 mM phenol, 1.0 g/L TiO_2, 1.0 mM Ni^{2+}, and pH 7.0). The solution pH was adjusted with a dilute solution of $HClO_4$ or NaOH. A suspension containing necessary components was stirred in the dark for 0.5 h, and then irradiated with a high pressure mercury lamp. The light intensity reaching the external surface of reactor was 4.50 mW cm^2, measured with a UVA irradiance meter. At given intervals, 2.0 mL of the suspension was withdrawn, and filtered through a 0.22 μm membrane. The filtrate was immediately analyzed by HPLC (high performance liquid chromatography) on a Dionex UltiMate 3000 (50% CH_3OH as eluent). TOC (total organic content) was analyzed on a TOC-V CPH TOC analyzer (Shimadzu).

2.4. Adsorption isotherm of Ni^{2+}

Measurement was carried out at 25 °C and in the dark. A suspension containing 2.0 g/L catalyst and a certain concentration of Ni^{2+} was stirred for 12 h, and then filtered through a 0.22 μm membrane. Through a complex with dimethylglyoxime [20], Ni^{2+} ions were analyzed at 550 nm on an Agilent 8453 UV–vis spectrophotometer.

2.5. Recycle test of Ni^{2+}

Reaction was performed with Pt/TiO_2 five times, in absence and presence of Ni^{2+}, respectively. For each run under similar conditions, two suspensions were prepared, which were A (100 mL, 2.0 g/L Pt/TiO_2, and pH 7.0), and B (100 mL, 2.0 g/L Pt/TiO_2, 1.0 mM Ni^{2+}, and pH 7.0). Each suspension was divided into two parts. One was continuously stirred in the dark. Another was mixed with 1.0 mL of phenol stock solution (11 mM), followed by stirring for 30 min, and irradiation with UV light. For A and B, total irradiation time was 70 and 15 min, respectively. During this period of time, five samples were taken out for analysis, and each of them was 2 mL. After that, the irradiated suspension was supplied with 10 mL of the un-irradiated suspension and 1 mL of phenol stock solution, followed by pH adjustment to initial pH 7.0. After stirred in the dark for 30 min, new suspension was irradiated again, and analyzed as described above.

2.6. (Photo)electrochemical measurement

A film working electrode was prepared by doctor blade method. A gel containing PVA (polyvinylalcohol) and TiO_2 or Pt/TiO_2 coated an indium-doped tin oxide (ITO) glass (Nippon Sheet Glass). To remove PVA, the film glass was annealed in air at 500 °C for 1 h. Then the glass was cut into several pieces. Each piece had an exposed area of 1.0 cm^2, and other part was sealed by epoxy resin. Measurements were carried out on a CHI660E Electrochemical Station (Chenhua, Shanghai), using a platinum gauze as counter electrode, and an Ag/AgCl as reference electrode. The working electrode was illuminated with a 500 W Xenon lamp, from the electrode/electrolyte side. The electrolyte was 0.5 M $NaClO_4$ (pH 7.0), and the scanning rate was 10 mV/s.

3. Results and discussion

3.1. Characterization

Solid was characterized with XRD, TEM, DRS, N_2 adsorption, and XPS, and the results are shown in Figure S1 of the Supporting Materials. In brief, TiO_2 and Pt/TiO_2 had XRD patterns, well matching that of anatase TiO_2 (PDF #65-5714), respectively. According to the strongest diffraction, two samples were similar in peak intensity, integrated area, and peak width at half height (Table S1). It means that TiO_2 phase remains unchanged after Pt deposition. In the TEM images, the TiO_2 particles were spherical-like, with a diameter of about 30 nm, either in absence or presence of Pt. In the adsorption—desorption isotherm of N_2, there was a hypothesis loop, indicative of mesopores present in samples. But the surface area, total pore volume, and average pore size of Pt/TiO_2 were slightly smaller than those of TiO_2, respectively. It means that the solid pores are partially occupied or blocked by Pt fine particles. In the DRS spectrum, there was an intensive absorption at wavelengths shorter than 400 nm region, assigned to the band-to-band transition of TiO_2. Through a Tauc plot, the band gap energy (E_g) for indirect transition was estimated to be 3.2 eV for both TiO_2 and Pt/TiO_2. In the XPS spectrum of Pt 4f, there were two peaks at 69.73 and 73.79 eV, assigned to Pt $4f_{7/2}$ and Pt $4f_{5/2}$ of Pt^0, respectively [21–24]. But the binding energy of Pt/TiO_2 was 0.77 eV lower than that of Pt/C (71.5 eV), due to the shift of electron density from TiO_2 to Pt [21,22]. These observations indicate that metallic Pt is deposited onto TiO_2, without obvious change in the crystal structure, crystallite size, and optical property of TiO_2 phase.

3.2. Photocatalytic degradation of phenol

In this study, $Ni(ClO_4)_2$ was used as Ni^{2+} source, because specific anions such as F^- and SO_4^{2-} have influence on TiO_2 photocatalysis [19,25]. Fig. 1A shows the results of phenol degradation on TiO_2 and Pt/TiO_2, measured in the absence and presence of 1 mM Ni^{2+}. Among the samples, the rates of phenol degradation were Pt/TiO_2 + Ni^{2+} > P25 > Pt/TiO_2 > TiO_2 + Ni^{2+} > TiO_2, where P25 is a mixture of anatase and rutile, and it is often used as a reference photocatalyst. To confirm the effect of Ni^{2+}, several experiments under UV light were performed. First, in a homogeneous solution of $Ni(ClO_4)_2$ or $NaClO_4$,

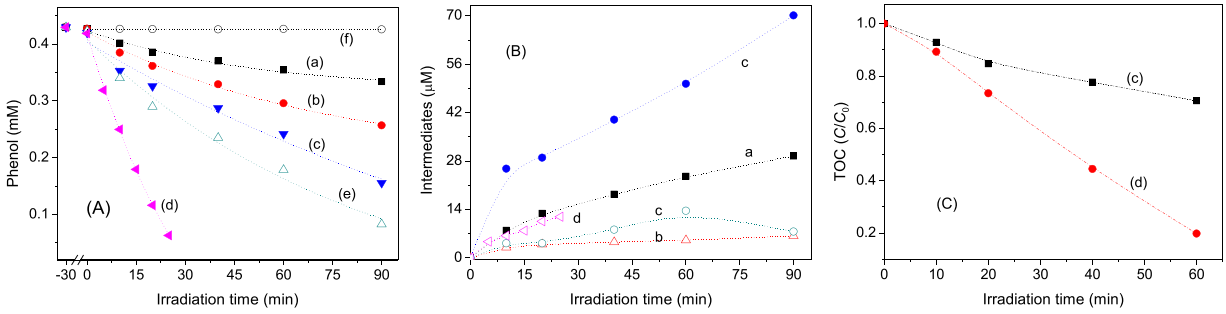

Fig. 1. (A) Phenol degradation over (a) TiO_2, (b) TiO_2 + Ni^{2+}, (c) Pt/TiO_2, (d) Pt/TiO_2 + Ni^{2+}, (e) P25 TiO_2, and (f) Ni^{2+}. (B) The corresponding formation of hydroquinone (solid symbols) and benzoquinone (open symbols), and (C) change of total organic content (TOC).

there was negligible decrease in phenol concentration. That is, phenol was stable against UV light, even in the presence of Ni^{2+}, Na^+, and ClO_4^-, respectively. Second, with TiO_2 or Pt/TiO_2 as photocatalyst, the addition of $NaClO_4$ did not change the rate of phenol degradation (Fig. S2A). Then the increased rate of phenol degradation on addition of Ni$(ClO_4)_2$ is surely due to the positive of Ni^{2+} cations, not ClO_4^- anions. Third, on addition of 1 mM Ni$(ClO_4)_2$, Ni$(NO_3)_2$, and $NiCl_2$, the rates of phenol degradation on TiO_2 were all increased, but Ni$(ClO_4)_2$ was more active than other nickel salts (Fig. S2B). These observations indicate that Ni^{2+} ions are beneficial to the photocatalytic degradation of phenol either on TiO_2 or Pt/TiO_2.

All of the time profiles for phenol degradation well fit the pseudo-first-order rate equation, and the resulting apparent constants (k_{obs}) are shown in Table 1. Such kinetics is often observed in TiO_2 photocatalysis, and attributed to the constant formation of reactive species under a fixed condition [26,27]. In the present work, phenol photolysis in aqueous solution and its adsorption on TiO_2 were both negligible. Then a large value of k_{obs} corresponds to a high concentration of reactive species produced. According to k_{obs}, one can say that the photocatalytic activity of Pt/TiO_2 is approximately 4 times that of TiO_2. This is ascribed to the formation of a Schottky barrier allowing electron transfer from TiO_2 to Pt [12,28], and/or due to the thermal catalysis of Pt for O_2 reduction [21]. Both of them would inhibit electron recombination with the holes, and hence promote the hole oxidation of phenol. On the addition of Ni^{2+}, strikingly, the photocatalytic activities of TiO_2 and Pt/TiO_2 increased by factors of 2.1 and 8.0, respectively. Moreover, the k_{obs} value of Pt/TiO_2 plus Ni^{2+} was 4.7 times the sum of individual k_{obs} (TiO_2 plus Ni^{2+}, and Pt/TiO_2). These observations indicate that for phenol degradation, Ni^{2+} ions are not only beneficial, but also have a cooperative effect with Pt, further improving the photocatalytic activity of TiO_2.

During phenol degradation, benzoquinone (BQ) and hydroquinone (HQ) were identified as main intermediates, and the results are shown in Fig. 1B. In the absence or presence of Ni^{2+}, total intermediates formed from Pt/TiO_2 were more than those produced from TiO_2 (Tables S2 and S3). This trend in intermediate production between two catalysts matches that in phenol degradation. However, with each catalyst, HQ was much more and less than BQ in the absence and presence of Ni^{2+}, respectively, whereas the total intermediates measured with Ni^{2+} were less than those obtained without Ni^{2+}. These observations imply that Ni^{2+} not only helps HQ transformation to BQ, but also helps BQ degradation into some intermediates. The total organic content (TOC) was measured, and the result obtained with Pt/TiO_2 is shown in Fig. 1C. As irradiation time increased, TOC decreased gradually. But the decay of TOC with time in presence of Ni^{2+} was faster than that in absence of Ni^{2+}. For example, on addition of Ni^{2+}, TOC removal yield at 60 min was greatly increased, from 30% to 80%. Moreover, on addition of Ni^{2+}, the mole ratio of total intermediates produced to phenol consumed was also notably decreased, from 29—35% to 3.3—7.2% (Tables S2 and S3). These observations indicate that Ni^{2+} ions are beneficial to both the photocatalytic oxidation and mineralization of phenol either on TiO_2 or Pt/TiO_2.

Table 1
Data of phenol degradation and Ni^{2+} adsorption.

Sample	Phenol k_{obs} (10^{-3} min^{-1})[a]		Ni^{2+} adsorption[b]	
	Without Ni^{2+}	With 1 mM Ni^{2+}	q_m (mmol/g)	K (mM^{-1})
TiO_2	2.55	5.41	0.204	24.1
Pt/TiO_2	10.2	73.3	0.197	25.8

[a] k_{obs}, apparent rate constant.
[b] q_m, the maximum amount of adsorption; K, adsorption constant.

3.3. Effect of variables

Fig. 2A shows the pH effect on the rate constants of phenol degradation over TiO_2 and Pt/TiO_2. In absence of Ni^{2+}, the rate of phenol degradation slightly increased with the suspension pH. In presence of 1 mM Ni^{2+}, however, the reaction rates greatly changed with the initial pH. A maximum reaction rate was observed at approximately pH 7.0, either from TiO_2 or Pt/TiO_2. Interestingly, the effect of Ni^{2+} was great at initial pH 7—10, but it was negligible at initial pH 3—6. This is presumably due to the pH-dependent adsorption of Ni^{2+} on solid. It is known that TiO_2 in aqueous solution is amphoteric [29]. Then the zeta potentials of solid in aqueous suspension at different pHs were measured, and the results are shown in Fig. S3A. At zero point of charge, the pH value (pH_{zpc}) was determined to be 5.56 for TiO_2, and 5.74 for Pt/TiO_2, respectively. That is, at a pH lower than pH_{zpc}, the surfaces of photocatalysts are positively charged, unfavorable to Ni^{2+} adsorption. In fact, as the suspension pH increased from 3 to 7, the amount of Ni^{2+} adsorbed on TiO_2 or Pt/TiO_2 in aqueous suspensions at pHs 3—7 greatly increased with pH (Fig. S3B). This is accordant with the reduced density of positive charges on solid. Since the pH-dependent change in the rate increase of phenol degradation matches that in the amount of Ni^{2+} adsorption, it follows that the observed positive effect of Ni$(ClO_4)_2$ is due to the Ni(II) species adsorbed on solid, rather than in solution. Moreover, there is also a distribution of Ni^{2+} and $NiOH^+$ in aqueous solution (Ni^{2+} + OH^- = $NiOH^+$, $K_f = 4.47 \times 10^5$) [30]. A theoretical calculation with 1 mM Ni^{2+} solution showed that the mole percent of Ni^{2+} and $NiOH^+$ decreased and increased, respectively, as the solution pH was increased (Fig. S4A). For examples, in aqueous solution at pH 7, there are 96% Ni^{2+} and 4% $NiOH^+$. In other words, the adsorbed Ni(II) species on solid in a weakly aqueous solution would be $NiOH^+$, which then takes part into the photocatalytic degradation of phenol.

At a suspension pH higher than 7, however, a green precipitate was formed, due to the hydrolysis of Ni^{2+} ions to Ni$(OH)_2$. According to the solubility product of Ni$(OH)_2$ in water ($K_{sp} = 7.94 \times 10^{-17}$) [30], a solution of 1 mM Ni^{2+} would give Ni$(OH)_2$ at a pH equal to and higher than 7.5. Since phenol degradation at pH 7 was faster than those at pH 8—10, it follows that on the oxide surface, $NiOH^+$ ions are more active

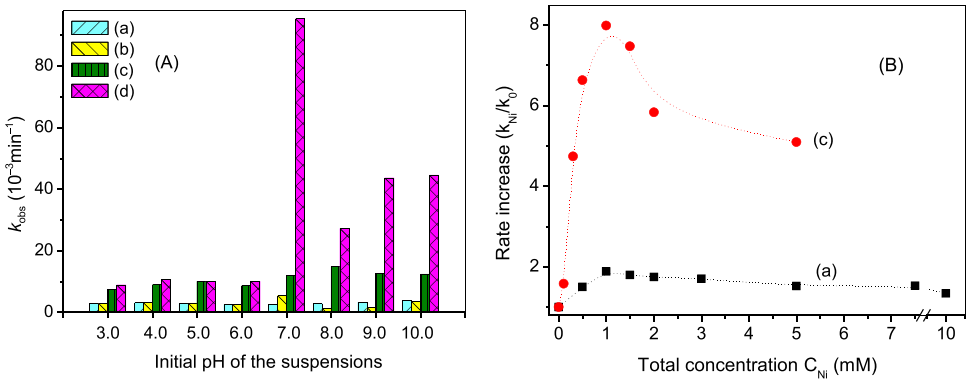

Fig. 2. (A) Effect of initial pH on the rate constant of phenol degradation (k_{obs}), measured in the presence of (a) TiO_2, (b) TiO_2 + 1.0 mM Ni^{2+}, (c) Pt/TiO_2, and (d) Pt/TiO_2 + 1.0 mM Ni^{2+}. (B) Effect of Ni^{2+} concentration on the rate increase (k_{Ni}/k_0), where k_0 and k_{Ni} represent the rate constants of phenol degradation at initial pH 7 in the absence and presence of Ni^{2+}, respectively.

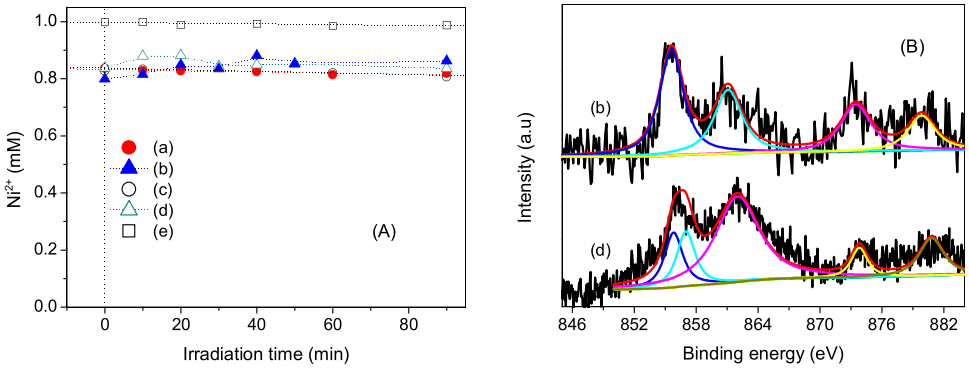

Fig. 3. (A) Time profiles of Ni^{2+} concentration in aqueous phase, under different conditions of (a) TiO_2 + Ni^{2+} + phenol, (b) Pt/TiO_2 + Ni^{2+} + phenol, (c) TiO_2 + Ni^{2+}, (d) Pt/TiO_2 + Ni^{2+}, and (e) Ni^{2+}. (B) XPS spectrum of Ni 2p, recorded from samples (b) and (d), after irradiation for 90 min.

than $Ni(OH)_2$, in participation of the photocatalytic reaction. In a comparison with the loosely deposited $Ni(OH)_2$ on TiO_2, the electrostatically adsorbed $NiOH^+$ on TiO_2 would have a stronger interaction, and hence a faster reaction with the irradiated TiO_2. The rate of phenol degradation at pH 8, lower than those at pHs 9 and 10, is probably due to incomplete deposition of a colloidal $Ni(OH)_2$ onto solid, causing light scattering, reducing the number of photons reaching TiO_2, and consequently decreasing the rate of photoreaction.

Fig. 2B shows the effect of Ni^{2+} concentration (C_{Ni}) at initial pH 7.0, where k_0 and k_{Ni} represent the apparent rate constants of phenol degradation measured in absence and presence of Ni^{2+}, respectively. As C_{Ni} increased, the ratio of k_{Ni} to k_0 increased initially, and then decreased. A maximum k_{Ni}/k_0 was observed around 1.0 mM Ni^{2+}, either from TiO_2 or Pt/TiO_2. However, the raise and decay of k_{Ni}/k_0 with C_{Ni}, observed from Pt/TiO_2, were faster than those, obtained from TiO_2, respectively. That is, the effect of Ni^{2+} to Pt/TiO_2 is larger than that to TiO_2. Note that in all of Ni^{2+} solutions at pH 7, there are always 96% Ni^{2+} and 4% $NiOH^+$ (Figure S4B). That is, the observed effect of C_{Ni} is not due to the change in the distribution of Ni species.

To understand the different effect of C_{Ni}, the adsorption isotherms of Ni^{2+} on solid in aqueous suspension at pH 7.0 were measured, and the results are shown in Fig. S3C. As the equilibrium concentration of Ni^{2+} in aqueous phase (C_{eq}) increased, the amount of Ni^{2+} adsorbed on solid (q) increased toward a limit. The isotherm well fit the Langmuir adsorption equation, $q/q_m = KC_{eq}/(1 + KC_{eq})$, where q_m is the maximum amount of adsorption, and K is adsorption constant. The q_m and K values of Pt/TiO_2 are slightly smaller and larger than those of TiO_2, respectively (Table 1). The former matches the change in solid surface area and pore volume (Table S1). The latter is probably indicative of a special interaction between Ni^{2+} and Pt. In the region of low C_{Ni}, there was a linear correlation between k_{Ni}/k_0 and q (Fig. 2B and S3B). This is in agreement with the above proposal that the positive effect of Ni^{2+} is due to the adsorbed $NiOH^+$ on solid. Interestingly, a maximum k_{Ni}/k_0 was observed at 1 mM Ni^{2+}, which occupied 50% of TiO_2 surface, and 58% of Pt/TiO_2, respectively. Beyond the optimum surface coverage, k_{Ni}/k_0 became to decrease with C_{Ni} for TiO_2. According to K_{sp}, in a solution at pH 7, $Ni(OH)_2$ is formed only when C_{Ni} is higher than 7.94 mM. Then the decreased rate of phenol degradation at 1—5 mM Ni^{2+} is due either to the green solution of Ni^{2+}, reducing the number of photons reaching photocatalyst, or to the adsorbed Ni species on solid, decreasing the amount of O_2 adsorption on photocatalyst. Both of them would slow down the photocatalytic reaction for phenol degradation. However, in the range of C_{Ni} examined (0.1—5 mM), the rates of phenol degradation on TiO_2 and Pt/TiO_2 are all larger than those without Ni^{2+}, respectively. These observations indicate that the adsorbed $NiOH^+$ species on TiO_2 and Pt/TiO_2 are indeed beneficial to the photocatalytic degradation of phenol.

3.4. Recycle behavior of Ni^{2+} ions

During phenol degradation, Ni^{2+} concentration in aqueous phase was monitored, and the results are shown in Fig. 3A. In the dark, about 18% of Ni^{2+} ions were adsorbed on solid. Under UV light, Ni^{2+} concentration did not change with time, on the average. At the same time, however, the suspension changed its color from white to pale brown, as observed notably from Pt/TiO_2 (Fig. S5A). Such color change is due to the formation of yellowish BQ from phenol degradation (Fig. 1B), and/or due to the change of solid chemical state. To clarify it, Pt/TiO_2 was collected, dried, and analyzed by XPS. In the spectrum of Pt 4f, no difference was observed between the dark and irradiated samples (Fig. S1C and S1D). In the spectrum of Ni 2p, there were two peaks at 855.3 and 873.1 eV (Fig. 3B), assigned to Ni $2p_{3/2}$ and Ni $2p_{1/2}$, respectively. But there was also no difference between the dark and irradiated samples (Fig. S6A and S6B). Moreover, both the peak position and separation (17.8 eV) of Ni 2p were similar to those for a $Ni(OH)_2$ powder [31], and a $Ni(OH)_2$ thick film on TiO_2 and Fe_2O_3 [32–35]. These observations indicate that during phenol degradation, Ni^{2+} ions remain unchanged, either in concentration or chemical state.

A question arose regarding how Ni^{2+} ions were beneficial to phenol degradation. To examine the fate of Ni^{2+}, experiment with Pt/TiO_2 and 1 mM Ni^{2+} was carried out in the absence of phenol. Under UV light, Ni^{2+} concentration in aqueous phase remained unchanged with time (Fig. 3A, open symbols). At the same time, the suspension changed its color from white to brown. But such color change in absence of phenol (Fig. S5B) was faster than that in presence of phenol (Fig. S5A). Control experiments with Pt/TiO_2 (Fig. S5C), and TiO_2 plus Ni^{2+} (Fig. S5D) showed negligible and slow color changes, respectively. These observations imply that a new Ni species is formed on the irradiated catalyst, which is reactive to phenol, but not to water. To identify it, Pt/TiO_2 was collected, dried, and analyzed by XPS. In the spectrum of Ni 2p, there was an obvious difference between the dark and irradiated samples (Fig. S6C and S6D). After light irradiation, the Ni $2p_{3/2}$ peak was shifted by 0.8 eV, together with a 1.0 eV increase in the peak width at half height. Since the peak was asymmetric, it was deconvoluted into two peaks at 855.8 and 857.0 eV, respectively (Fig. 3B). The former matches that for Ni $2p_{3/2}$ of Ni^{2+}. The latter is assigned to Ni $2p_{3/2}$ of Ni^{3+}, as observed from a photoelectrochemically oxidized $Ni(OH)_2$ thick film on Fe_2O_3 [34,35]. But the XPS peaks due to NiO (854.3 eV) and Ni^0 (852.7 eV) were absent in the present sample [32,33,36,37]. These observations indicate that the adsorbed $NiOH^+$ ions on solid under UV light are oxidized to a Ni^{3+} species, mostly in the form of NiOOH. Then NiOOH oxidizes phenol to regenerate Ni^{2+}, followed by the re-adsorption of Ni^{2+} onto solid. Since NiOOH is surface bound, and not reactive to H_2O, Ni^{2+} concentration in aqueous phase remains unchanged with irradiation time, either in the absence or presence of phenol (Fig. 3A).

To examine the recycle behavior of Ni^{2+}, phenol degradation on Pt/TiO_2 was repeated five times, and the results are shown in Fig. 4A. For the reactions in the absence and presence of 1 mM Ni^{2+}, total irradiation time was fixed to be 70 and 15 min, respectively. In each run, phenol degradation with Ni^{2+} was always faster than that without Ni^{2+}. But from one run to another, the reaction rate gradually decreased, either in the absence or presence of Ni^{2+} (Table S4). This is mainly due to organic intermediates formed and accumulated in the reactor, competing with phenol for reactive species. However, from the first run to last, the ratio of k_{obs} in presence of Ni^{2+} to that in absence of Ni^{2+} remained nearly unchanged. It implies that Ni^{2+} ions are stable during the five repeated test. Fig. 4B and C show the time profiles for HQ and BQ formation. From one run to another, the intermediates gradually accumulated in the reactor. After the last run, total intermediates, formed in absence and presence of Ni^{2+}, were 60 and 20 μM, respectively. But they were all much less than total phenol disappeared (1.55 mM without Ni^{2+}, and 1.30 mM with Ni^{2+}). These observations indicate that Ni^{2+} ions can be repeatedly used for phenol degradation.

3.5. (Photo)electrochemical measurement

To further understand the effect of Ni^{2+}, the electron reduction of O_2 and the hole oxidation of phenol were examined independently. Fig. 5 shows the electrochemical reduction of O_2 in a 0.5 M $NaClO_4$ at pH 7. As the applied potential swept negatively, the dark current increased. At given potential, the electrode current under air was much larger than that under N_2. This is indicative of O_2 reduction being dominant process under air. By using a literature method [38], the onset potential of O_2 reduction was estimated, which was —0.152 and —0.142 V *vs.* AgCl/Ag for TiO_2 and Pt/TiO_2, respectively. On addition of 1 mM Ni^{2+}, the onset potentials of TiO_2 and Pt/TiO_2 negatively shifted to be —0.164 and —0.156 V *vs.* AgCl/Ag, respectively. Meanwhile, the electrode current was decreased, the degree of which was larger with TiO_2 than that with Pt/TiO_2. Regardless of Ni^{2+} present or not, moreover, the current of O_2 reduction on Pt/TiO_2 was always much larger than that on TiO_2. A more positive onset potential, and a larger current correspond to an easier reduction of O_2. These observations indicate that Pt efficiently catalyzes O_2 reduction [21], but Ni^{2+} ions are negative to O_2 reduction, either on TiO_2 or Pt/TiO_2. The inhibitory effect of Ni^{2+} on O_2 reduction is ascribed to the reduced amount of O_2 adsorption on the electrode, as proposed above for the observed decrease in the rate of phenol degradation with C_{Ni} at high C_{Ni} (Fig. 2B). Since Pt acts as electron traps and promotes O_2 reduction, such detrimental effect of Ni^{2+} for O_2 reduction on Pt/TiO_2 electrode is less serious than that on TiO_2 electrode.

Fig. 6 shows the photoelectrochemical oxidation of water and phenol on TiO_2 and Pt/TiO_2 film electrodes in a 0.5 M $NaClO_4$ at pH 7, measured in absence and presence of 1 mM Ni^{2+}. Before experiment, the electrolyte was purged with N_2, and then the cell was closed. In all cases, the electrode photocurrent increased, as the applied potential swept positively. This is due to the improved efficiency of charge separation for the hole reaction on the working electrode. But the effects of Ni^{2+} on water and phenol oxidation are different and complicated. In absence of phenol, both TiO_2 and Pt/TiO_2 electrodes showed a negative shift in onset potential on addition of Ni^{2+}. This is due to Ni^{2+} oxidation easier than water oxidation, as observed from a $Ni(OH)_2$ film on Fe_2O_3 photoanode [35]. To confirm it, the dark voltage-current curves for TiO_2 and Pt/TiO_2 electrodes were measured under N_2 in a 0.5 M $NaClO_4$ at pH 7, and the results are shown in Fig. S7A and 7B. With each electrode, the potential onset of water oxidation was 0.95 V *vs.* AgCl/Ag. In presence of 1 mM Ni^{2+}, the onset potential shifted to 0.80 V *vs.* AgCl/Ag. Such potential at pH 7 was reasonably more positive than a cyclic voltammetry potential of 0.70 V *vs.* AgCl/Ag, obtained at pH 10 from a $Ni(OH)_2$ deposited Pt/TiO_2 electrode (Fig. S7C). These observations confirm that the Ni^{2+}-caused negative shift in onset potential is due to Ni^{2+} oxidation, rather than H_2O oxidation. On the other hand, the photocurrents of TiO_2 and Pt/TiO_2 electrodes on addition of Ni^{2+} were decreased and increased, respectively. The decreased photocurrent of TiO_2 is due to brown NiOOH produced, which absorbs light, and reduce the number of photons reaching TiO_2. The increased photocurrent of Pt/TiO_2 is due to the hole oxidation of H_2O_2, formed from the Pt catalyzed reduction of O_2 (note that O_2 results from water oxidation). In absence or presence of Ni^{2+}, moreover, the photocurrent of Pt/TiO_2 was much smaller than that of TiO_2. This is

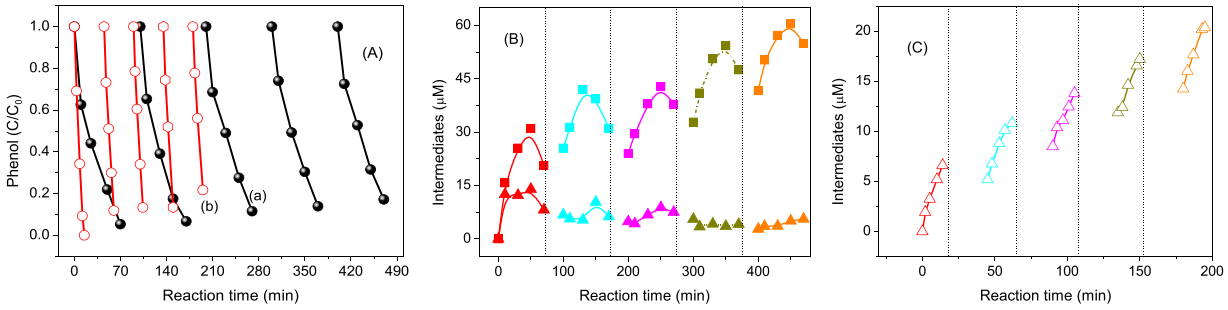

Fig. 4. (A) Phenol degradation on Pt/TiO_2 (a) in absence, and (b) presence of Ni^{2+}. The formation of hydroquinone (square symbols) and benzoquinone (triangle symbols), (B) without, and (b) with Ni^{2+}. Initial conditions of each run: 2.0 g/L catalyst, 0.215 mM phenol, 1 mM Ni^{2+}, and pH 7.

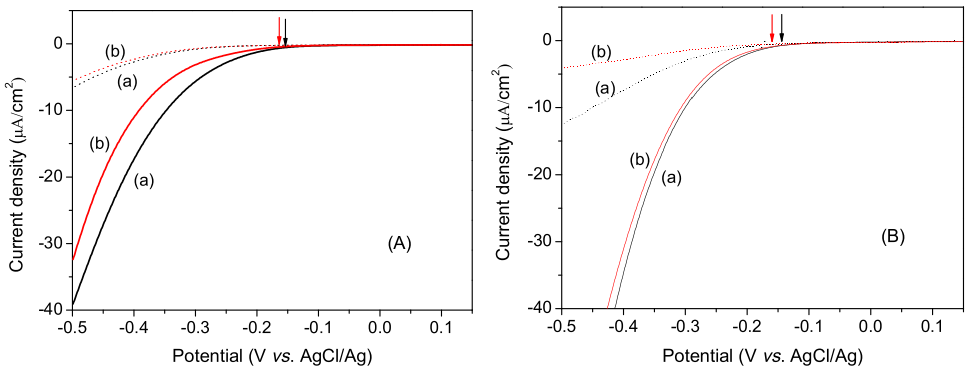

Fig. 5. Dark current-voltage curves of (A) TiO_2, and (B) Pt/TiO_2 film electrodes, measured under N_2 (dotted lines) and air (solid lines), (a) in the absence, and (b) presence of 1.0 mM Ni^{2+}.

ascribed to the electrons trapping by Pt, slowing down the electron flow to generate photocurrent [13].

In the presence of phenol, the onset potentials of TiO_2 and Pt/TiO_2 were also negatively shifted, on the addition of Ni^{2+}. This is ascribed to the hole oxidation of Ni^{2+} easier than phenol oxidation. But at an external potential more positive than approximately 0 V *vs*. AgCl/Ag, both of the electrodes showed an increased photocurrent, different from those observed in the absence of phenol. Accordingly, the increased photocurrent of each electrode on addition of Ni^{2+} is due to phenol oxidation by NiOOH. At an applied potential more negative than approximately 0 V *vs*. AgCl/Ag, the electron reduction of NiOOH to Ni^{2+} might also occur, with a rate higher than that of phenol oxidation by NiOOH. That is, there is a competition between the formation and reduction of NiOOH on the electrode. As a result, the increased photocurrent due to phenol oxidation by NiOOH is observed only after the photoelectrons are efficiently removed. These observations indicate that NiOOH formed on irradiated TiO_2 or Pt/TiO_2 is reactive to phenol, but not to water.

3.6. Possible mechanism

To understand the effect of Ni^{2+}, one needs to know the band gap energy (E_g), conduction band edge potential (E_{cb}), and valence band edge potential (E_{vb}) of semiconductor, where $E_g = E_{vb} - E_{cb}$. For n-type semiconductor such as TiO_2, E_{cb} is close to E_{fb}, the flat band potential. In this study, E_{cb} was measured through a Mott—Schotty plot, and it was then used to calculate E_{cb} and E_{vb} (see details in Fig. S8). Experiment was performed in a 0.5 M $NaClO_4$ at pH 7, and the results are shown in Table 2. In the absence of Ni^{2+}, both TiO_2 and Pt/TiO_2 have E_{cb} more negative than the potential of $O_2/O_2^{\bullet-}$ couple (—0.33 V vs NHE) [8,9], whereas their E_{vb} are more positive than the potential of phenol$^{+\bullet}$/phenol couple (1.03 V vs. NHE) [10]. Then in thermodynamics the electron reduction of O_2 and the hole oxidation of phenol are all possible. On the addition of Ni^{2+}, both TiO_2 and Pt/TiO_2 showed a negative shift in band edge potential. But their electrons to reduce O_2 and their holes to oxidize phenol are still allowed in thermodynamics. As a result, phenol degradation was observed, either in the absence or presence of Ni^{2+} (Fig. 1A).

Table 2
Band edge potentials for semiconductors in a 0.5 M $NaClO_4$ at pH 7[a].

Sample	E_{fb} (V, NHE)	E_{cb} (V, NHE)	E_{vb} (V, NHE)
TiO_2	—0.34 (—0.42)	—0.47 (—0.52)	2.73 (2.68)
Pt/TiO_2	—0.42 (—0.59)	—0.55 (—0.71)	2.65 (2.49)

[a] Bracket data represent ones measured in presence of 1 mM $Ni(ClO_4)_2$. E_{fb}, flat band potential; E_{cb}, conduction band edge potential; E_{vb}, conduction band edge potential. Details in experiment and calculation method are shown in Fig. S8.

In aqueous solution at pH 7, the electrochemical oxidation of Ni^{2+} occurred around 0.80 V *vs.* AgCl/Ag, or 1.0 V *vs*. NHE (Fig. S7). This potential is less positive than E_{vb} of TiO_2 and Pt/TiO_2, respectively. Then in thermodynamics, the hole oxidation of Ni^{2+} on two photocatalysts are both possible. In fact, the photocatalytic formation of NiOOH on Pt/TiO_2 in absence of phenol was observed by XPS (Fig. 3B). On the other hand, the potential for water oxidation to O_2 is 0.82 V *vs*. NHE. This potential is less positive than E_{vb} of two semiconductors (2.7 V *vs*. NHE), as well as the potential for Ni^{2+} oxidation (1.0 V vs. NHE). In practice, water oxidation by the photoholes of TiO_2 and Pt/TiO_2 were both observed (Fig. 6), but water oxidation by NiOOH was not observed (Fig. 3B). The non-reactivity of NiOOH toward water oxidation is also inferred from literature work. A photoelectrochemically oxidized $Ni(OH)_2$ thick film on TiO_2 can persist its brown color in air for several days [32,39]. Nevertheless, the larger photocurrent of $Ni(OH)_2/Fe_2O_3$ than that of Fe_2O_3 is ascribed to the oxidation of water by Ni^{IV} species, rather than by Ni^{III} [34,35].

The NiOOH produced from the hole oxidation of $NiOH^+$ can oxidize phenol, HQ and BQ (Figs. 1 and 4). Then Ni^{2+} ions are regenerated,

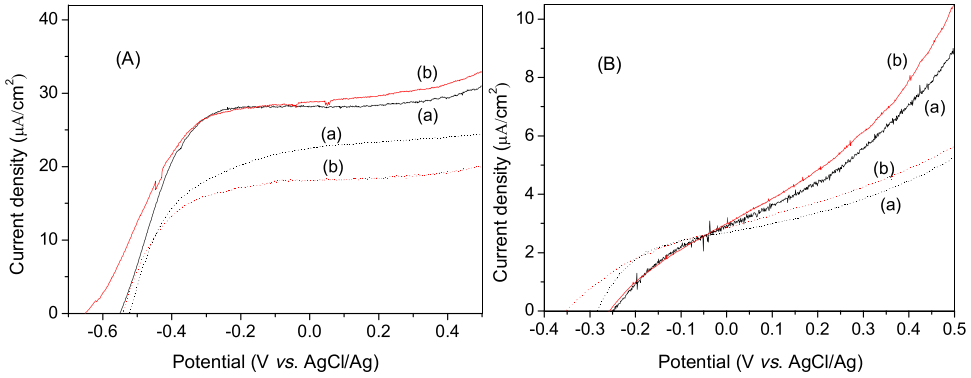

Fig. 6. Photoelectrochemical oxidation of water (dotted lines) and 0.43 mM phenol (solid lines) on (A) TiO_2, and (B) Pt/TiO_2 film electrodes under N_2 in 0.5 M $NaClO_4$, measured (a) without Ni^{2+}, and (b) with 1 mM Ni^{2+}. Note than the same electrode was used for (a) and (b), but different one was used for phenol and water oxidation, respectively.

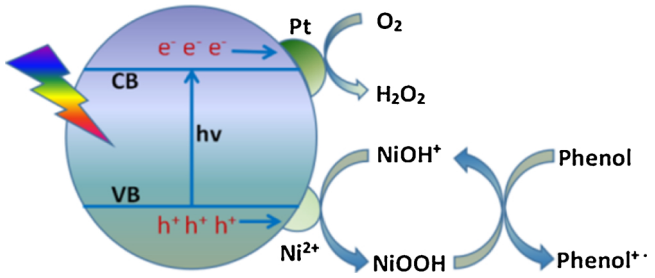

Scheme 1. A possible mechanism for the mutual effect of Pt and $NiOH^+$ on TiO_2 photocatalysis.

followed by subsequent hole oxidization to NiOOH. As a result, Ni^{2+} concentration in solution remains unchanged during phenol degradation (Fig. 3A). In aqueous solution, Ni^{2+} ions highly adsorb onto TiO_2 (0.2 mmol/g, Table 1), as compared with phenol (less than 0.01 mmol/g). Then, more photoholes of TiO_2 are consumed by Ni^{2+} ions, and more photoelectrons of TiO_2 are available to O_2 reduction. As a result, the efficiency of charge separation is improved, and the rate of phenol oxidation is increased.

In TiO_2 photocatalysis, the electrons and holes are photogenerated and consumed in pairs. Since Pt efficiently catalyzes O_2 reduction, the hole oxidation of phenol on Pt/TiO_2 is faster than that on TiO_2, as observed in absence of Ni^{2+} (Fig. 1A). The Pt-mediated electron transfer would promote the $NiOH^+$-mediated hole transfer, and vice versa. As a result, the efficiency of charge separation is further improved, and the rate increase of phenol degradation on addition of Ni^{2+} is much larger with Pt/TiO_2 than that with TiO_2 (Fig. 2B). On the other hand, the amount of O_2 adsorption on TiO_2 in aqueous solution is reduced on addition of Ni^{2+}, due to surface occupation of $NiOH^+$ (Fig. 5). The reduced amount of O_2 on photocatalyst would then result into a decreased rate of O_2 reduction, and hence a decreased rate of phenol degradation. In practice, however, the rate of phenol degradation increased with C_{Ni} at low C_{Ni} (Fig. 2B). These observations further indicate that the hole oxidation of Ni^{2+} is more efficient than the hole oxidation of phenol. At high C_{Ni}, the inhibitory effect of Ni^{2+} on O_2 adsorption becomes dominant, and the rate of phenol degradation then decreased with C_{Ni} (Fig. 2B). Since Pt/TiO_2 is much more active than TiO_2, the Ni^{2+} caused rate decrease of phenol degradation on Pt/TiO_2 is also much larger than that on TiO_2 (Fig. 2B). In other words, the effect of Pt and $NiOH^+$ mutually cooperate, greatly changing the photocatalytic activity of TiO_2 for O_2 reduction and phenol oxidation, as outlined in Scheme 1.

Furthermore, an alternative mechanism of Ni^0 as cocatalyst has been proposed in the literature [33,36]. For the photocatalytic production of H_2 in presence of excess ethanol, a $Ni(OH)_2$-deposited P25 TiO_2 was much more active than P25 TiO_2. The observed positive effect of $Ni(OH)_2$ is ascribed to the reduction of $Ni(OH)_2$ into Ni^0 clusters, followed by the Ni-catalyzed reduction of H^+ to H_2. In our sample, however, no Ni^0 was observed by XPS (Fig. 3B). To verify this pathway, experiment with an aqueous suspension containing 2 g/L of TiO_2 and 10% of CH_3OH in volume was carried out under N_2. After light irradiation for 2 h, the amounts of H_2, produced from TiO_2 and TiO_2 plus 1 mM Ni^{2+}, were 322 and 4506 μmol/g, respectively. Meanwhile, the TiO_2 suspension changed its color from white to blue, but the suspension containing Ni^{2+} changed its color from white to grey, with some black particles in the position of a LED lamp (Fig. S9). The former is due to the formation and accumulation of Ti^{III} species, because the electron reduction of protons is much slower than the hole oxidation of CH_3OH. The black particles are probably Ni^0 clusters. In aqueous solution at pH 0, the Ni^{2+}/Ni couple has a potential (—0.25 V vs. NHE) more negative than E_{CB} of anatase TiO_2 (—0.12 V vs. NHE) [7]. Then in thermodynamics, the reduction of Ni^{2+} by the photoelectrons of TiO_2 is impossible. We speculate that the observed black Ni particles result from the reduction of Ni^{2+} by H_2 produced *in situ* under N_2. In the present work, therefore, a Ni^{3+} species formed on the surface of TiO_2 from the hole oxidation of $NiOH^+$ under air is responsible for the observed enhancement of phenol degradation on addition of Ni^{2+}.

4. Conclusions

A simple addition of Ni^{2+} ions into the aerated aqueous suspension of TiO_2 can result into great enhancement in the rates of phenol oxidation and mineralization under UV light. A maximum reaction rate is located around initial pH 7, with Ni^{2+} ions occupying half the surface of TiO_2 at approximately 50%. Through a theoretical calculation, the observed positive effect of Ni^{2+} is ascribed to the strongly adsorbed $NiOH^+$ ions on TiO_2, which are more active than the loosely deposited $Ni(OH)_2$ on TiO_2. During phenol degradation, Ni^{2+} ions act as co-catalyst, without change in concentration. Since Pt efficiently catalyzes O_2 reduction, not only phenol degradation on Pt/TiO_2 is much faster than that on TiO_2, but also the effect of Ni^{2+} ions to Pt/TiO_2 is larger than that to TiO_2. On the irradiated Pt/TiO_2, moreover, there is formed a Ni^{3+} species, not Ni^0. With the aid of (photo)electrochemical measurement, it is proposed that NiOOH is formed from the hole oxidation of $NiOH^+$, followed by phenol oxidation to regenerate Ni^{2+}. Then the $NiOH^+$-mediated hole promotes the Pt-mediated electron transfer, and vice versa. As a result, the efficiency of charge separation is improved, and the rate of phenol degradation is increased. Since Ni^{2+} ions are often present in water, and they are also cheap in cost, this work has a good prospect of using Ni^{2+} ions as the hole mediator of organic oxidation on different semiconductors.

Declaration of Competing Interest

None.

Acknowledgment

This work was supported by the Funds for Creative Research Group of NSFC (No. 21621005). We thank Prof. B. Chen and D. Lin for help in TOC measurement.

Appendix A. Supplementary data

Supplementary material related to this article can be found, in the online version, at doi:https://doi.org/10.1016/j.apcatb.2019.117903.

References

[1] K. Takanabe, Photocatalytic water splitting: quantitative approaches toward photocatalyst by design, ACS Catal. 7 (2017) 8006–8022.
[2] J. Ran, M. Jaroniec, S.Z. Qiao, Cocatalysts in semiconductor-based photocatalytic CO_2 reduction: achievements, challenges, and opportunities, Adv. Mater 30 (31) (2018) 1704649.
[3] Z. Xing, J. Zhang, Y. Cui, J. Yin, T. Zhao, J. Kuang, Z. Xiu, N. Wan, W. Zhou, Recent advances in floating TiO_2-based photocatalysts for environmental application, Appl. Catal. B 225 (2018) 452–467.
[4] S. Chandrasekaran, C. Bowen, P. Zhang, Z. Li, Q. Yuan, X. Ren, L. Deng, Spinel photocatalysts for environmental remediation, hydrogen generation, CO_2 reduction and photoelectrochemical water splitting, J. Mater. Chem. A 6 (2018) 11078–11104.
[5] S.K. Loeb, P.J.J. Alvarez, J.A. Brame, E.L. Cates, W. Choi, J. Crittenden, D.D. Dionysiou, Q. Li, G. Li-Puma, X. Quan, D.L. Sedlak, T. David Waite, P. Westerhoff, J.-H. Kim, The technology horizon for photocatalytic water treatment: sunrise or sunset? Environ. Sci. Technol. 53 (2019) 2937–2947.
[6] O. Carp, C.L. Huisman, A. Reller, Photoinduced reactivity of titanium dioxide, Prog. Solid State Chem. 32 (2004) 33–177.
[7] T. Tachikawa, M. Fujitsuka, T. Majima, Mechanistic insight into the TiO_2 photocatalytic reactions: design of new photocatalysts, J. Phys. Chem. C 111 (2007) 5259–5275.
[8] D.T. Sawyer, J.S. Valentine, How super is superoxide, Acc. Chem. Res. 14 (1981) 393–400.
[9] I.A. Weinstock, Homogeneous-phase electron-transfer reactions of polyoxometalates, Chem. Rev. 98 (1998) 113–170.

[10] C. Li, M.Z. Hoffman, One-electron redox potentials of phenols in aqueous solution, J. Phys. Chem. B 103 (1999) 6653–6656.
[11] A. Naldoni, M. Altomare, G. Zoppellaro, N. Liu, S. Kment, R. Zboril, P. Schmuki, Photocatalysis with reduced TiO_2: from black TiO_2 to cocatalyst-free hydrogen production, ACS Catal. 9 (2019) 345–364.
[12] D. Hufschmidt, D. Bahemann, J.J. Testa, C.A. Emilio, M.I. Litter, Enhancement of the photocatalytic activity of various TiO_2 materials by platinisation, J. Photochem. Photobiol. A 148 (2002) 223–231.
[13] J.S. Lee, W. Choi, Photocatalytic reactivity of surface platinized TiO_2: substrate specificity and the effect of Pt oxidation state, J. Phys. Chem. B 109 (2005) 7399–7406.
[14] L. Wan, J. Sheng, H. Chen, Y. Xu, Different recycle behavior of Cu^{2+} and Fe^{3+}ions for phenol photodegradation over TiO_2 and WO_3, J. Hazard. Mater. 262 (2013) 114–120.
[15] X. Xiong, X. Zhang, Y. Xu, Concentration dependent effect of $CuCl_2$ on the photocatalytic degradation of phenol over anatase, rutile and brookite TiO_2, RSC Adv. 6 (2016) 38169–38175.
[16] X. Zhang, X. Xiong, L. Wan, Y. Xu, Effect of a Co-based oxygen-evolving catalyst on TiO_2-Photocatalyzed organic oxidation, Langmuir 33 (2017) 8165–8173.
[17] N.S. Begum, H. Ahmed, K.R. Gunashekar, Effects of Ni doping on photocatalytic activity of TiO_2 thin films prepared by liquid phase deposition technique, Bull. Mater. Sci. 31 (2008) 747–751.
[18] M.I. Litter, Heterogeneous photocatalysis transition metal ions in photocatalytic systems, Appl. Catal. B 23 (1999) 89–114.
[19] C. Minero, G. Mariella, V. Maurino, E. Pelizzetti, Photocatalytic transformation of organic compounds in the presence of inorganic anions. 1. hydroxyl-mediated and direct electron-transfer reactions of phenol on A titanium dioxide-fluoride system, Langmuir 16 (2000) 2632–2641.
[20] H.R. Rajabi, S. Razmpour, Synthesis, characterization and application of ion imprinted polymeric nanobeads for highly selective preconcentration and spectrophotometric determination of Ni^{2+} ion in water samples, Spectrochim. Acta A 153 (2016) 45–52.
[21] D. Huang, B. Zhang, J. Bai, Y. Zhang, G. Wittstock, M. Wang, Y. Shen, Pt catalyst supported within TiO_2 mesoporous films for oxygen reduction reaction, Electrochim. Acta 130 (2014) 97–103.
[22] V.A. Saveleva, V. Papaefthimiou, M.K. Daletou, W.H. Doh, C. Ulhaq-Bouillet, M. Diebold, S. Zafeiratos, E.R. Savinova, Operando near ambient pressure XPS (NAP-XPS) study of the Pt electrochemical oxidation in H_2O and H_2O/O_2 ambients, J. Phys. Chem. C 120 (2016) 15930–15940.
[23] L. Di, X. Zhang, Z. Xu, K. Wang, Atmospheric-pressure cold plasma for preparation of high performance Pt/TiO_2 photocatalyst and its mechanism, Plasma Chem. Plasma Process. 34 (2013) 301–311.
[24] A.V. Vorontsov, E.N. Savinov, Z.S. Jin, Influence of the form of photodeposited platinum on titania upon its photocatalytic activity in CO and acetone oxidation, J. Photochem. Photobiol. A 125 (1999) 113–117.
[25] X. Zhang, X. Xiong, Y. Xu, Brookite TiO_2 photocatalyzed degradation of phenol in presence of phosphate, fluoride, sulfate and borate anions, RSC Adv. 6 (2016) 61830–61836.
[26] D.F. Ollis, Kinetics of liquid phase photocatalyzed reactions: an illuminating approach, J. Phys. Chem. B 109 (2005) 2439–2444.
[27] A.V. Emeline, V.K. Ryabchuk, N. Serpone, Dogmas and misconceptions in heterogeneous photocatalysis. some enlightened reflections, J. Phys. Chem. B 109 (2005) 18515–18521.
[28] J. Yu, L. Qi, M. Jaroniec, Hydrogen production by photocatalytic water splitting over Pt/TiO_2 nanosheets with exposed (001) facets, J. Phys. Chem. C 114 (2010) 13118–13125.
[29] B. Ohtani, Y. Okugawa, S. Nishimoto, T. Kagiya, Photocatalytic activity of TiO_2 powders suspended in aqueous silver-nitrate solution-correlation with pH-dependent surface-structures, J. Phys. Chem. 91 (1987) 3550–3555.
[30] S.V. Mattigod, D. Rai, A.R. Felmy, L.F. Rao, Solubility and solubility product of crystalline $Ni(OH)_2$, J. Solution Chem. 26 (1997) 391–403.
[31] S. Yu, Z. Li, X. Fan, J. Li, F. Zhan, X. Li, Y. Tao, C. Tung, L. Wu, Vectorial electron transfer for improved hydrogen evolution by mercaptopropionic-acid-regulated CdSe quantum-dots-TiO_2 -$Ni(OH)_2$ assembly, ChemSusChem 8 (2015) 642–649.
[32] Y. Takahashi, T. Tatsuma, Oxidative energy storage ability of a TiO_2-$Ni(OH)_2$ bilayer photocatalyst, Langmuir 21 (2015) 12357–12361.
[33] J. Yu, Y. Hai, B. Cheng, Enhanced photocatalytic H_2-production activity of TiO_2 by $Ni(OH)_2$ cluster modification, J. Phys. Chem. C 115 (2011) 4953–4958.
[34] Q. Liu, F. Cao, F. Wu, H. Lu, L. Li, Ultrathin amorphous $Ni(OH)_2$ nanosheets on ultrathinα-Fe_2O_3 films for improved photoelectrochemical water oxidation, Adv. Mater. Interfaces 3 (2016) 1600256.
[35] G. Wang, Y. Ling, X. Lu, T. Zhai, F. Qian, Y. Tong, Y. Li, A mechanistic study into the catalytic effect of $Ni(OH)_2$on hematite for photoelectrochemical water oxidation, Nanoscale 5 (2013) 4129–4133.
[36] W. Wang, S. Liu, L. Nie, B. Cheng, J. Yu, Enhanced photocatalytic H_2-production activity of TiO_2 using $Ni(NO_3)_2$ as an additive, Phys. Chem. Chem. Phys. 15 (2013) 12033–12039.
[37] J. Ran, J. Yu, M. Jaroniec, $Ni(OH)_2$ modified CdS nanorods for highly efficient visible-light-driven photocatalytic H_2 generation, Green Chem. 13 (2011) 2708.
[38] W.F. Chen, K. Sasaki, C. Ma, A.I. Frenkel, N. Marinkovic, J.T. Muckerman, Y. Zhu, R.R. Adzic, Hydrogen-evolution catalysts based on non-noble metal nickel-molybdenum nitride nanosheets, Angew. Chem. Int. Ed. Engl. 51 (2012) 6131–6135.
[39] R. Kostecki, T. Richardson, D. McLarnon, Photochemical and photoelectrochemical behavior of a novel $TiO_2/Ni(OH)_2$ electrode, J. Electrochem. Soc. 145 (1998) 2380–2385.